

Article

Leaching of Rare Earth Elements from Central Appalachian Coal Seam Underclays

Scott N. Montross ^{1,2,*}, Jonathan Yang ^{1,3}, James Britton ⁴, Mark McKoy ⁵ and Circe Verba ¹

¹ National Energy Technology Laboratory, Albany, OR 97321, USA; Jonathan.yang@netl.doe.gov (J.Y.); Circe.Verba@netl.doe.gov (C.V.)

² Leidos Research Support Team, Albany, OR 97321, USA

³ Oak Ridge Institute for Science and Education, Oak Ridge, TN 37830, USA

⁴ West Virginia Geological and Economic Survey, Morgantown, WV 26507, USA; britton@geosrv.wvnet.edu

⁵ National Energy Technology Laboratory, Morgantown, WV 26507, USA; Mark.McKoy@netl.doe.gov

* Correspondence: Scott.Montross@netl.doe.gov

Received: 1 May 2020; Accepted: 23 June 2020; Published: 26 June 2020



Abstract: Rare earth elements (REE) are necessary for advanced technological and energy applications. To support the emerging need, it is necessary to identify new domestic sources of REE and technologies to separate and recover saleable REE product in a safe and economical manner. Underclay rock associated with Central Appalachian coal seams and prevalent in coal utilization waste products is an alternative source of REE to hard rock ores that are mainly composed of highly refractory REE-bearing minerals. This study utilizes a suite of analytical techniques and benchtop leaching tests to characterize the properties and leachability of the coal seam underclays sampled. Laboratory bench-top and flow-through reactor leaching experiments were conducted on underclay rock powders to produce a pregnant leach solution (PLS) that has relatively low concentrations of gangue elements Al, Si, Fe, and Th and is amenable to further processing steps to recover and produce purified REE product. The leaching method described here uses a chelating agent, the citrate anion, to solubilize elements that are adsorbed, or weakly bonded to the surface of clay minerals or other mineral solid phases in the rock. The citrate PLS produced from leaching specific underclay powders contains relatively higher concentrations of REE and lower concentrations of gangue elements compared to PLS produced from sequential digestion using ammonium sulfate and mineral acids. Citrate solution leaching of underclay produces a PLS with lower concentrations of gangue elements and higher concentrations of REE than achieved with hydrochloric acid or sulfuric acid. The results provide a preliminary assessment of the types of REE-bearing minerals and potential leachability of coal seam underclays from the Central Appalachian basin.

Keywords: rare earth elements; coal utilization byproducts; pregnant leach solution; underclay; organic acid

1. Introduction

Rare earth elements (REE) are essential for the development of low-carbon, renewable energy technologies. In the United States (U.S.), a lack of domestic REE production is forcing end-users in energy, high-end technology, and manufacturing sectors to seek overseas sources. Exploration and production of new domestic sources of REE and critical minerals (CM) is essential to meet future demands. The U.S. Department of Energy report—2017 Report to Congress on Rare Earth Elements from Coal and Coal Utilization Byproducts—on rare earth elements from coal and coal byproducts outlines the strategic plan for expanding the U.S. REE reserve base [1]. The plan calls for identification of coal and coal byproducts with the highest known concentration of REE and the development of

cost-effective separation technologies to recover the resource. A diversified REE product slate that includes recovery of REE from domestic coal byproducts and various types of sedimentary geologic materials can contribute to supply security and help to limit risks to market disruptions [1,2].

Production of REE in the United States, primarily sourced from bastnaesite and other accessory minerals, has increased between 2018–2019 from 18,000 to 26,000 tons, but is low compared to Chinese production (132,000 tons) [2]. The United States' domestic coal and coal utilization byproducts (CUB) are nevertheless promising sources of recoverable REE [1–6]. The term CUB includes a range of materials that are produced during coal utilization [1,3–6]. Coal mining waste rock and coal preparation plant refuse are two types of byproduct that contain underclay, a clay-rich sedimentary rock that is found adjacent to a coal seam. Underclay is commonly categorized as roof or floor rock and it is exposed and sometimes excavated during the mining of a coal seam.

Clay-rich horizons in Central Appalachian (CentApp) coal seams, for example, commonly contain higher concentrations of REE than the coal or other non-clay bearing rock adjacent to the coal seam [3,4]. In the CentApp region, there are approximately 840 coal refuse piles that overlie nearly 40 square kilometers of abandoned mines and coal fields. The amount of coal refuse in Pennsylvania alone is estimated to be 1.5×10^9 cubic meters [7]. Waste refuse piles, which plausibly contain a high percentage of clay minerals, may be heap leached or processed with limited beneficiation techniques (e.g., crushing and grinding, calcining, roasting, and floatation), compared to mineral bound ore. REE and CM can be leached from produced and stockpiled waste materials. With the availability of potential resource material, numerous studies have investigated REE recovery from coal-related materials, including coal fly ash [8,9], coal middlings [5,10], and underclays [3,4,10]. Underclays have an increased resource potential [4] as the rock is often subjected to previous diagenetic events and natural processes that transport and concentrate REE and CM in forms that may be easier to extract, compared to minerals bound in crystalline rock. Ease of extraction makes this type of material a more promising geologic source of REE and CM.

Organic acids and their degradation products provide ligands and chelating agents for heavy metals [11]. The citric acid-citrate system forms a relatively stable complex with alkaline earth metals [12] as well as heavy metals and lanthanides. The citric acid molecule is composed of one alpha position hydroxyl and carboxyl group and two beta position carboxylic acid groups, together the molecule contains at least seven potential O-donor sites that are capable of coordinating metal ions [12,13]. Carboxyl groups of citric acid have been shown to complex with both bivalent and trivalent metal ions in biological systems [13,14] and during interaction with alkaline earth metal ions [12].

Effects of organic acid on the leaching process of REE from ion-adsorbed clays was investigated by Wang et al. [15]. The leaching experiments by Wang et al. [15] showed REE recovery using citric acid was highest (10.4 mmol/kg) at pH range 3.5–4.0. The experiments were conducted at varying pH with the same carboxylic group concentration of 10^{-4} mol/L. Rare earth element concentrations decreased in the solutions with increasing pH (from 2–6). Increased pH should lead to greater acid dissociation because of pKa shifts increasing the number of complexation sites for REE on the organic ligands. The results confirm that organic anions, including anions of citric acid, can act as assistant leaching agents both through the complexation of REE in solution and the interaction with the clay surface to promote changes in the zeta potential of the clay. This process can lead to greater leaching of sorbed cations from the clay surface or for better dispersion of individual clay grains [15].

Citric acid anion recovery of REE from coal seam underclay is a promising method that may liberate higher concentrations of ion exchangeable REE from the clay compared to traditional lixiviants such as ammonium sulfate or sodium chloride. We chose to investigate the influence of organic acids on the recovery of exchangeable, or weakly bonded, REE ions from the surfaces of clay grains, as well as liberation of the nonexchangeable (stronger bonded) REE ions. Our selective approach of using pH buffered organic acid-based solutions amended with ionic constituents (e.g., $(\text{NH}_4)_2\text{SO}_4$ or NaCl) is designed to isolate and recover the exchangeable REE fraction type through partial dissolution of the

clay matrix. The approach is based on previous studies which have shown that optimum recovery of REE adsorbed on clay minerals using ionic lixiviants occurs at the 3–4 pH range [15–17].

A mildly acidic organic acid-based ionic recovery solution with the presence of a monovalent salt likely liberates clay surface adsorbed REE and some inorganic REE mineral phases embedded in the clay matrix. The leaching solution may be pH buffered for optimum recovery from different clay mineral assemblages. Clay grains have a high surface area typically with a negative net charge. Exchangeable and nonexchangeable ions are present on the surface of clay grains. The amount of cation exchange capacity (CEC) or anion exchange capacity (AEC) is dependent on the clay mineral type or presence of organic matter. Exchangeable ions are weakly held in contact with the clay solution and are readily replaced by ions in solution. Positively charged ions, such as Al^{3+} , Ca^{2+} , K^+ , and REE^{3+} , may be present on clay surfaces as exchangeable ions. Nonexchangeable ions are typically adsorbed by strong bonds or held in inaccessible places within the clay matrix (e.g., K^+ between layers of illite). The use of organic acids can potentially increase the recovery of REE from clay-rich rocks by: (a) Maintaining a balanced charge on clay surfaces and increasing cation exchange capacity (CEC); (b) selectively dissolving matrix rock and increasing pore space connectivity and transmissivity of fluids; and (c) solubilizing phosphate bound REE [18,19].

Rozelle et al. [3] identified clay-rich ore deposits that contain up to 90% of the total REE in the rock, bound as ion-adsorbed REE, with the balance existing as colloids (e.g., Fe, Mn-oxides) and crystalline minerals (e.g., REE-phosphates). In China, about 10,000 tons of rare earth oxide (REO) concentrate are produced annually from weathered elution-deposits derived from lateritic weathering of granitic rock and in situ aqueous mining yields ~200 tons of REE annually [17]. This study characterizes and tests the leaching behavior of underclay rock from geologic formations associated with coal production in West Virginia, Pennsylvania, and Ohio.

2. Materials and Methods

2.1. Sample Preparation

The National Energy Technology Laboratory Research and Innovation Center (NETL-RIC) obtained underclay core samples from the West Virginia Geological and Economic Survey (WVGES) (Figure 1). The core samples were taken from strata associated with production coal seams—Lower Freeport, Middle Kittanning, and Pittsburgh No.5—in West Virginia.



Figure 1. Photographs of as-received underclay core samples examined in this study. Information and descriptions of rock from the core samples are shown in Table 1.

A sample of approximately 200 g was either cut from the core or collected as chips and pieces. Each sample was pulverized first using a small jaw crusher then Zr-Ti lined shatter box to reduce the grain size to 149 μm or less. A mortar and pestle was used to hand-grind the material until it all passed through a 100 mesh (<149 μm) sieve. After grinding and sieving the powdered sample was homogenized using the cone and quarter technique [20]. The homogenized sample was split into specific subsamples for X-ray diffraction (30 g), elemental analysis (3 g), sequential digest (5 g), and leaching tests (0.5 g and ~40 g). Sample preparation for X-ray diffraction analysis included an additional step. The homogenized sample was ground for 60 s in a micronizing mill to achieve a grain size of <65 μm . The subsamples for the different analyses and tests were stored in chemical-free paper envelopes in a nitrogen purged desiccator until needed. The goal for sampling and sample preparation was to create a bulk homogenized underclay powder that could be used to test the recovery of REE from clay-rich material using different leaching solutions composed of organic acid anions. Bulk analysis and characterization of each sample was conducted to determine basic mineralogical and physical properties of the material. Rock chips or slices of core (3 cm \times 2 cm) were used for electron microscopy imaging and X-ray microanalysis. Contextual information about the samples and core descriptions of the material are shown in Table 1.

Table 1. Sample information and core descriptions for underclay samples.

Sample ID	Material Type Formation	Depth (ft)	Core Description
UC-01	Underclay, shale Lower Freeport	1352.0–1352.5	Dark black to gray; fine grain matrix with visible pyrite and calcite cement; irregular sharp wavy contact. Directly underlies base of lower Freeport coal.
UC-02	Flint-clay, underclay Middle Kittanning	1463.0–1463.5	Medium to light gray/olive green rock fragments. Sub angular fine to medium clasts; few fine root traces and plant debris; few fine to medium black shale and coal streaks; clear lower contact.
UC-03	Underclay Pittsburgh	740.5–741.0	Medium gray and olive yellow-brown; common fine distinct olive mottles; few fine faint black mottles; few fine faint red mottles; clear lower contact.
UC-06	Paleosol, seat earth Lower Freeport	712.6–713.0	Pistachio green; extremely brecciated; paleosol; spiderweb calcite cement; siderite banding; soft sediment deformation structures present.

2.2. Scanning Electron Microscopy and X-Ray Microanalysis

Thin section and epoxy-mounted samples were evaporatively coated with carbon and imaged with a field emission scanning electron microscope (FE-SEM, FEI Inspect F) equipped with an energy-dispersive X-ray spectrometer (EDS, Oxford Instruments, Abingdon, UK). SEM imaging and EDS analysis was done at 20 kV, ~100 nA; a working distance of 10.4 mm, beam aperture 3, and spot size 5.0–5.5 nm. The entire area of the sample—thin section or epoxy mounted rock slice—was viewed frame by frame in x and y directions at low magnification (300 \times) in backscattered electron mode (BSE). Electron microscope images and EDS data were collected from single spots and full fields of view at multiple locations within the sample. Large area images (4 mm²) with corresponding EDS maps were collected and constructed using the automate function in the Oxford INCA SEM-EDS software package (Version 5.05, Oxford Instruments, Abingdon, UK). Standards-based quantitative EDS was accomplished using REE-phosphate standards REEP25-15+ FC (Astimex Standards Ltd., Toronto, ON, Canada) and REE-oxide standard #489 (Gellar Analytical, Topsfield, MA, USA) for all analyses. Standard block #489 is certified to ISO 9001 and 17025 standards. Putative mineral phase identifications were made using images and elemental data from SEM-EDS analysis.

2.3. X-Ray Diffraction

Bulk mineralogy of rock samples was determined by X-ray diffraction (XRD) of randomly oriented powder mounts. Each sample was powdered to $<63\ \mu\text{m}$ using a micronizing mill. The powdered samples were spiked with 10 wt. % ZnO and mounted on an automatic 6-position sample changer equipped with a sample spinner. XRD patterns were collected using a Rigaku III Ultima diffractometer with Cu K-alpha radiation at 40 kV and 44 mA from 3.0–65.0 degrees-two-theta with a step size of 0.02° at 2.4 s. Initial peak alignments and identifications, and mineral IDs were made via comparison of the diffraction peaks against the ICDD-4 database using HighScore Plus XRD software (Version 3.0, Malvern PANalytical Ltd., Malvern, UK). Basic Rietveld fitting was performed using the software to quantify mineral percentages and estimate amorphous content (wt. %). Semi-quantitative analysis of crystalline components and mineral phase identifications were done by diffraction pattern analysis using the RockJock 7.0 computer program (U.S. Geological Survey, Boulder, CO, USA) [21].

Oriented mounts were prepared for clay identification by XRD analysis following the methods outlined in the U.S. Geological Survey (USGS) Open file report 01-041 [22]. The prepared mounts of each sample were scanned with a Rigaku III Ultima diffractometer (Rigaku, Tokyo, Japan) with Cu K-alpha radiation at 40 kV and 44 mA from 2.0–30.0 degrees-two-theta with a step size of 0.02° at 0.5° per minute. After the initial scan, the samples were treated sequentially with ethylene glycol and two separate heat treatments (400 and 550 °C). The samples were scanned after each treatment. Phase IDs, peak alignments, and mineral identifications of clay mineral peaks were made via comparison of the diffraction peaks against the ICDD-4 database using MDI Jade 6.0 XRD software (MDI Jade, Livermore, CA, USA). Diffraction patterns for untreated and treated samples were compared using Jade and basic Rietveld fitting was performed using the software to quantify mineral percentages. Presence of specific clay mineral phases was determined by changes in diffraction peak patterns across treatments following the identification flow chart in the USGS report [22].

2.4. Particle Size

Particle size analyses were completed on unreacted and reacted solid samples using a Malvern Mastersizer2000 (Malvern PANalytical Ltd., Malvern, UK) following procedures outlined in Sperazza et al. [23]. Briefly, $\sim 5.5\ \text{g/L}$ sodium hexametaphosphate was added to the solid samples as a dispersant and vortexed. The resulting slurry was then added to the sample introduction unit and the laser obscuration value adjusted to fall between 10–20% by adding tap water or additional sample. For unreacted samples, 60 s of ultrasonication was applied in the pre-measurement routine. For reacted samples, ultrasonication was turned off to preserve the particle size distribution from the reaction. Standardization and accuracy of measurements was monitored with QA standard QAS3002 (15–150 μm) from Malvern. Analytical procedure and results are shown in the Supplementary Materials.

2.5. Sequential Acid Digestion

Underclay powders were reacted sequentially using ammonium sulfate $(\text{NH}_4)_2\text{SO}_4$, hydrochloric acid (HCl), sulfuric acid (H_2SO_4) and the residual solids were subjected to lithium borate (LiBO_2) fusion and digestion. The procedure was designed to operationally evaluate common lixivants used in commercial leaching and extraction of REE from geologic materials [24] and to provide a first-order comparison to leaching with organic acid-based reagents. The reagents and conditions for each step of the sequential digest are shown in Table 2. Dry, powdered sample was combined with different reagents and mixed in polypropylene tubes on a rotator at 25 rpm or stirred and heated in 100-mL Teflon beakers on a magnetic hot plate. At the end of each step the extraction solutions were separated by centrifugation $3500\times g$ for 20 min. The extraction solution was collected from the centrifuge tube with a syringe and the liquid passed through a $0.45\ \mu\text{m}$ nylon filter and collected for analysis. Major, trace, and rare earth element concentrations in the liquids collected were determined by inductively coupled plasma optical emission spectroscopy (ICP-OES) and mass spectroscopy (ICP-MS) following

the methods in Bank et al. [25]. Post extraction solids were collected by centrifugation and washed by rinsing the solids with ~30 mL of MilliQ, mixing solids and water on the rotator for 5 min and then separated by centrifugation (3500× g, 20 min). The wash step was repeated three times. The washed solids were dried at 60 °C overnight and weighed for dry weight. Weight loss for each step was always less than 5%. The steps were repeated for each solution. The remaining solid material was collected for LiBO₂ fusion and digestion [25] and reported as residual.

Table 2. Extraction reagents and conditions used in sequential extraction. Concentration of reagents shown in mol/L (M). Mass of starting.

Step	Reagent/Target Fraction	Solids (%)	Temperature (°C)	Time (h)	pH
1	0.5 M (NH ₄) ₂ SO ₄ Exchangeable	1	22	4	5.0
2	1 M HCl Colloid	1	22	24	1.0
3	1.2 M H ₂ SO ₄ Colloid + Mineral	1	70	1	0.86
4	LiBO ₂ -Digestion Mineral + Residual	200 mg	-	-	-

2.6. Citrate Leaching of REE

Benchtop leaching experiments were conducted on subsamples of underclay powders using various formulations of a water based leaching solution. The composition of each solution tested and a list of samples and conditions for each leach are shown in Table 3. The solutions were composed of combination of citric acid, sodium chloride, and conjugate buffer salt sodium citrate tribasic dihydrate (HOC(COONa)(CH₂COONa)₂·2H₂O). Initial benchtop tests were conducted using rock powders from sample UC-01, 02, 03, and 06 and liquid–solid ratio of 1% solids (e.g., 50 mL of leaching solution—0.5 g of powder). The powders and solution were combined in 50 mL polypropylene tubes and mixed using a tube mixer. Subsequent testing was performed on sample UC-02 using 20 g of powder and 200 mL of citrate leaching solution (10% solids). The test was conducted to (a) to verify the 10% slurry was properly mixed during the leaching steps, and (b) produce a PLS from a larger sample of material. Element concentrations in pregnant leach solutions (PLS) were determined by ICP-OES and ICP-MS. All leaching solutions contained a citrate concentration [citric acid + Na-citrate] of 0.1 mol/L (M) (See Table 3). In some cases, (NH₄)₂SO₄, or NaCl was added to the organic acid solution to provide an additional source of ions for ion exchange. Solutions were buffered to pH 3, 4, 5, or 6 using a mixture of citric acid and sodium citrate at a final concentration of 0.1 M citrate. The leaching solutions were mixed with a 0.5 g subsample of rock powder that was originally collected from the bulk homogenized sample (see above section) dried and powdered (<150 μm, 100 mesh) underclay sample in a 50 mL polypropylene centrifuge tube. The tubes were mixed on a rotational mixer for a range of times from 4–24 h at room temperature. The solution was separated from the slurry at the end of the leaching time by centrifugation (3500 rpm for 25 min.). The liquid was recovered from the tube with a syringe then passed through a 0.45-micron nylon filter. The solution pH was measured, and the remaining liquid sample was analyzed by ICP-MS at the NETL Pittsburgh Analytical Laboratory following the methods in Bank et al. [25].

Table 3. Leaching solutions and conditions used in benchtop experiments.

Solution ID	Composition	Samples Tested	Solid (%)	Temp (°C)/Time (h)	pH
RS-1	0.1 M Citrate * ($C_6H_5O_7^{3-}$ + 0.5 M Ammonium Sulfate $(NH_4)_2SO_4$)	UC-02, UC-06	1	22/4	5.1
RS-2	0.1 M Citrate * + 0.5 M Sodium Chloride (NaCl)	UC-01, UC-02, UC-06	1, 10	22/24	3.5
RS-3	0.1 M Citrate *	UC-02, UC-06	1	22/24	2.0
RS-4	0.5 M Sodium Chloride (NaCl)	UC-01, UC-02, UC-06	1	22/24	5.0
RS-7	0.1 M Citric acid + Na-Citrate ($NaC_6H_5O_7^{3-}$) + 0.5 M NaCl	UC-01, UC-02, UC-03, UC-06	1	21/24	3.0–6.0

* Citrate from citric acid.

2.7. Flow Through

Powdered samples and fractured core samples were flooded with leaching solution RS-2 (see Table 3) a citrate buffered solution amended with NaCl. Fluid flow was established for time periods of 1–24 h. Hold-in times, referring to the length of time the solution is in contact with the sample (either powder or core) without flow, were varied from 20 min to 5 days. For the powdered clay samples, saturated flow was initially established and maintained for 5–6 h, after which flow was discontinued and sampling proceeded in a stepwise function at discrete time points of 6 h, 7 h, 24 h, and 5 days from the initial contact of fluid with the sample. Detailed descriptions of equipment, experimental setup, and the experimental parameters are found in the Supplementary Materials section on flow-through experiments.

3. Results and Discussion

3.1. Characterization of Underclay

The concentration of elements in the underclay samples, expressed as oxides, are shown in Table 4. Silicon (as SiO_2) and Al (as Al_2O_3) are the dominant cations in all samples. The range of Al_2O_3 concentrations (see Table 4) indicate the material comes from highly weathered crustal materials [26]. Additionally, low Ca, Na, and K values are also indicative of highly weathered horizons or zones of intense leaching. The exception is the Ca concentration in UC-06, with calcite and siderite cement present throughout the rock matrix and visible in hand specimens (See Figure 1).

Table 4. Concentration of major cations as oxides (wt. %) in underclay samples.

Sample	Al	Ca	Fe	K	Mg	Na	P	Si	Ti	Zr
UC-01	18.5	0.4	9.0	3.1	1.6	0.3	0.1	62.8	0.9	<0.04
UC-02	28.0	0.8	1.7	3.2	0.5	0.4	0.1	63.3	1.4	<0.04
UC-03	18.9	0.7	4.5	4.0	1.2	0.6	0.0	68.4	0.9	<0.04
UC-06	24.9	5.4	2.4	3.9	0.4	0.4	0.4	65.3	1.2	<0.04

The extensive network of carbonate cement throughout the clay matrix is due to late diagenesis. The presence of diagenetic calcite in sample UC-06 results in a high concentration of Ca (5.4%) compared to the other underclay samples analyzed <1.0%. Rare earth element concentrations in each sample are shown in Table 5. The four samples have REE concentrations ranging from 262–353 mg/kg (See Table 5). The results reported in Table 5 are from the powdered and homogenized samples used for characterization, sequential digest, and 1% solids leaching tests. The results from a subsequent analysis of powder samples used in the leaching tests under different pH conditions are shown in Table S1

of the Supplementary Materials. Sample UC-02, a flint clay/underclay from the Middle Kittanning formation, had the highest REE concentration.

Table 5. Rare earth element concentrations (mg/kg) in West Virginia coal underclay samples. Values are reported on a whole sample basis.

Sample	La	Ce	Pr	Nd	Sm	Eu	Gd	Tb	Dy	Y	Ho	Er	Tm	Yb	Lu	ΣREE
UC-01	51.0	103.1	12.6	49.5	10.0	2.1	10.9	1.2	8.9	43.8	1.7	4.6	0.6	4.1	0.6	305
UC-02	82.9	119.3	13.2	45.4	9.4	2.8	9.7	1.0	8.0	50.3	1.5	4.3	0.6	4.2	0.6	353
UC-03	58.3	74.5	8.7	32.9	7.3	2.1	7.2	0.7	6.7	54.0	1.2	3.7	0.6	3.8	0.5	262
UC-06	71.3	102.1	9.7	30.9	7.1	1.9	6.0	0.4	5.1	35.4	0.9	2.9	0.4	3.0	0.5	278

Scanning electron microscope images of polished samples (see Figure 2) and various powdered samples (data not shown) were used to evaluate the composition and texture of the rock samples. SEM images and EDS results were used to make putative identifications of primary and secondary minerals in the samples, including the REE-bearing phases present. Rare earth element phosphate minerals were observed in all samples using SEM backscatter mode. The predominant REE-bearing mineral phases observed were rhabdophane, apatite, churchite, monazite, xenotime, and crandallite sp. Examples of REE-bearing minerals observed in the underclay samples analyzed are shown in Figure 2. Yang et al. [27] provides a comprehensive characterization of all REE-bearing minerals in the samples discussed here, as well as other underclay samples from West Virginia coal seam strata.

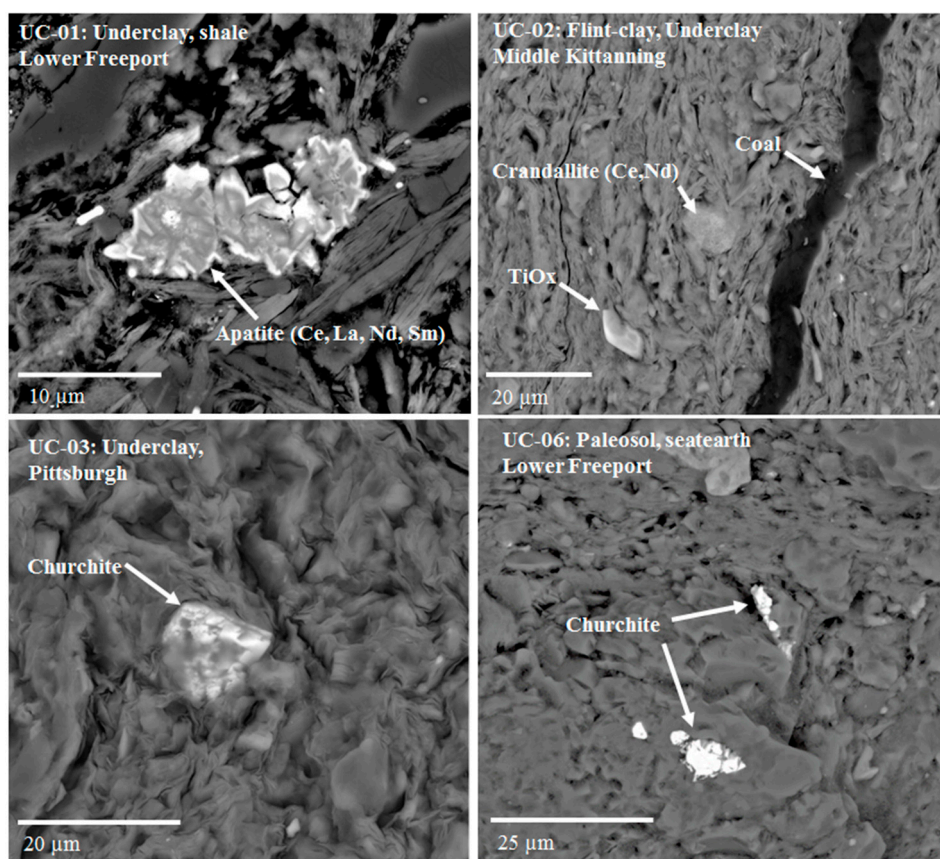


Figure 2. SEM micrographs of rock matrix and examples of rare earth elements (REE)-bearing minerals present in West Virginia underclay samples.

In sample UC-04 trace concentrations (1–4 wt. %) of Ce, La, and Nd were detected in grain-coating clay associated with pore filling framboidal pyrite and pyrite cement. Sample UC-02 contained Ce, La, Nd associated with aluminum phosphate (AlPO_4) mineral grains that were dispersed throughout

the rock matrix and have a similar chemical composition and morphology to the mineral crandallite, a hydrous aluminum phosphate. Crandallite contains LREE, Ba, and Sr and is present throughout the clay matrix as 5–50- μm sized crystals that oval to round in grain mount samples and appear as spongy, porous in thin section (Figure 2, upper right). A summary of the REE-bearing minerals identified in the samples and general observations of texture and other mineral phases present in the samples are shown in Table 6.

Table 6. General characterization results from SEM-EDS analysis.

Sample ID	REE-Bearing Minerals Identified	General Observations
UC-01	Apatite in pore space contains Ce, La, Nd REE phosphate grains with Ce, La, Nd, Sm, and Eu up to 20 μm long, also contain U/Th. Ce, La, and Nd detected in clay coating on framboidal pyrite. Ytterbium detected in pore filling pyrite cement.	Abundant pyrite in bands and isolated matrix grains Large euhedral pyrite grains (up to 50 μm) in matrix and as pore filling cements. Apatite grains contain ~1–3 wt. % U and Th.
UC-02	Ce, La, Nd phosphate (rhabdophane) and monazite) in clay pore space. Y, Gd, Dy, Er, Yb phosphate (xenotime) grains present in clay pore space. Range of size 1–10 μm long. Xenotime grains bound in massive iron oxide. Ce, La, Nd associated with aluminum phosphate (AlPO_4) dispersed throughout the rock matrix. Aluminum phosphate grains with similar chemical composition and morphology of the mineral crandallite. Crandallite present throughout the matrix as 5–50 μm size grains.	Abundant Ti Oxide with Hf (0.5 wt. %) and Sc (0.25 to 0.5 wt. %). Aluminum phosphate grains present. AlPO_4 contains equimolar concentrations of S, Sr, Ba, and REE (Ce, La, Nd, Sm). Stoichiometrically constant with the mineral crandallite an illite conversion product. Massive iron oxide. Mixed Cu, Se, Pb sulfides Plant root fossils
UC-03	Ce, La, Nd phosphate (rhabdophane or monazite) mineral grains in clay. Y phosphate (churchite or xenotime) grains in matrix.	Sample contains abundant Fe-oxide and Ti oxide. Fe oxide band collocated within coal layer. Zircon present. Clay matrix composed of illite and smectite. Abundant quartz
UC-06	Monazite present as large crystals 10–25 microns. Monazite contains up to 5.0 wt. % U/Th. Xenotime and monazite present as embedded grains within siderite or calcite. Cementation by Ca/P mineral phase with LREE detectable using EDS.	Abundant pore filling and pore lining clay. Matrix clay composed of fibrous, tubular morphology typical of Halloysite and platy particles resembling kaolinite. Diagenetic spider web calcite, banded siderite, and pore filling clay, Calcium phosphate mineralization Pyrite, barite, zircon, rutile, and galena present in the matrix. Light grey zones have high quartz content, lack extensive carbonate cementation. Dark grey zones contain massive siderite and calcite.

3.2. XRD Results

Analysis of diffraction patterns collected from randomly oriented and oriented powders showed that predominant crystalline non-clay components are quartz, calcite, and ilmenite. Illite and smectite are the most abundant clay minerals in the samples. Halloysite is present in minor (5–7%) abundance in all samples except UC-03. Clay minerals make up more than 55% of the bulk material in each sample. Semi-quantitative results for all non-clay and clay minerals identified are shown in the Table S2 in the Supplementary Materials. The samples are all composed of two-component mixed clays from the groups Kaolin (kaolinite and Halloysite) and Mica (illite). Kaolinite and halloysite were identified by evaluating changes to the 7 Å XRD peak present in the scans. In all samples the peak remained unchanged or there was a small increase in d-spacing following glycol treatment, both of which are attributed to the presence of kaolinite or halloysite. The distinguishing treatment was the destruction of the 7 Å XRD peak after heating to 550 °C. Further confirmation of the presence and classification of kaolinite and halloysite were made using electron micrographs. Kaolinite displays a hexagonal

morphology whereas halloysite has a tubular morphology. Analysis of SEM images confirms the presence of grains with hexagonal and tubular morphology. Illite was confirmed through the presence of a 10 Å XRD peak that remains unchanged by glycol and heat treatments.

3.3. Leaching of Rare Earth Elements from Underclay

The results of the sequential extraction of underclay powders and other leaching tests conducted on the samples in this study show that REEs are distributed across different mineral phases in the underclay. The results provided a basic screening of the distribution of REE in the bulk samples, specifically we were interested in the fraction of REE that was in the exchangeable phase. Other authors have presented results on ion-exchangeable clay from CentApp coal seam strata [2,18] and the results are not consistent across units in the basin [2,18,25]. Heterogeneity likely exists between individual clay units at the formation scale and plausibly within core samples collected from specific units. The samples may not be representative of an entire formation or basin, however, the results presented here are meaningful to evaluating different leaching solutions to recover REE from the material. The results of basic characterization efforts and leaching tests provide valuable information on not only the mineralogy and nature of REE-bearing minerals in the clay, but how the material responds to leaching with citrate solutions. In order to mature this technology and raise to a higher readiness level (TRL), currently at TRL 4-5, both the type and scale of sampling must be reconsidered, and the amount of material tested (e.g., scale) will have to be increased several fold. This is necessary due to the prevalence of heterogeneity and spatial variability of elements in geologic materials, as well as the presence of hot spots in such materials and within specific areas [28].

The samples discussed here and in Yang et al. [27] were taken from existing core samples. The characterization and analysis results reported here are from subsamples taken from the bulk, homogenized material prepared for the leaching tests. The results of basic sequential digest of the material, which can be considered a step-wise leaching test, are compared to the results of leaching using citrate. The results of the leaching tests are significant to evaluating alternative lixiviants (e.g., citric acid-citrate) and to compare the results to standard conventional mineral acid or salt leaches. The characteristics of the new solution, at minimum, should leach the ion-exchangeable fraction of REE from the samples, not produce excess liquid or solid hazardous waste, and be amenable to downstream processing to separate and recover REE in its pure form. Our leaching tests and demonstration of sorbent capture of REE from the citrate leachate demonstrate the potential of this technology.

We trialed a suite of different organic acids (e.g., acetic, indole-3-acetic, citrate) and formulations during our initial testing and development of an organic acid based lixiviant for recovering REE from clay [29]. Based on initial results we chose to pursue further testing and optimization of a citrate-based solution. A majority of the REE in the underclay samples analyzed here are bound in the residual phase (Table 7) and not extractable by exchange, or dissolution using 1 M HCl, or warm (70 °C) 1.2 M H₂SO₄. The complete set of analytical results for the sequential digests are shown in the Table S3 in the Supplementary Materials.

Table 7. Fraction of REE in pregnant leach solution (PLS) from sequential digestion of underclay powders. Values reported as percent of total REE leached from the solid sample.

Sample	(NH ₄) ₂ SO ₄ Exchangeable	HCl Extractable	H ₂ SO ₄ Extractable	Residual
UC-01	0.3	12.1	8.2	79
UC-02	7.5	19.0	6.8	67
UC-03	4.9	31.1	20.7	43
UC-06	1.3	10.1	3.5	85

The (NH₄)₂SO₄ exchangeable fraction of REE in the samples ranged from 0.3–7.5% and are low but generally fall within a range of other published values for ion-exchangeable REE in CentApp coal and coal byproducts [6,29,30], with the exception of the values reported by Rozelle et al. [2].

Underclay from the Middle Kittanning formation (MKT)—sample ID UC-02—and from the Pittsburgh coal seam—sample ID UC-03—contained the highest concentrations of $(\text{NH}_4)_2\text{SO}_4$ exchangeable and HCl extractable REE of the samples tested. Both samples contain ~25–35% of the total REE in the exchangeable and HCl leached fraction (Figure 3). This fraction is likely comprised of REE bound to the surface of clay minerals, carbonates, and Fe-oxides. While the remaining REE is bound to phosphatic minerals or within the structure of more recalcitrant phases and may only be recovered using hot sulfuric acid or more destructive dissolution techniques such as microwave digestion or treatment with hydrofluoric acid. The concentration of REE in the HCl extracts may be higher in these samples due to the abundance of metal oxides that may bind colloidal ions or carbonate that may have ion adsorbed/exchangeable REE (See Table 8). The concentration of REE and gangue elements in leachates recovered from sequential extraction were compared to bench-top leaching experiments with citrate, and the results are shown in Figure 3 and Table 8. Ammonium sulfate used for recovery of ion exchangeable leached ~10 μg of REE or approximately 7% of the total REE present in UC-02 (Figure 3 and Table 8), other samples tested had low recovery (<10% of the total REE) when using ammonium sulfate. Citrate leaching using a cycle of citrate solution amended with NaCl (pH 5) leached ~45 μg of REE into the PLS. This amount correlates to nearly 33% of the total REE in the clay sample. Two different slurry concentrations using sample UC-02, 1 and 10%, were leached with citrate + NaCl. The results of the comparison are shown in Table S5.

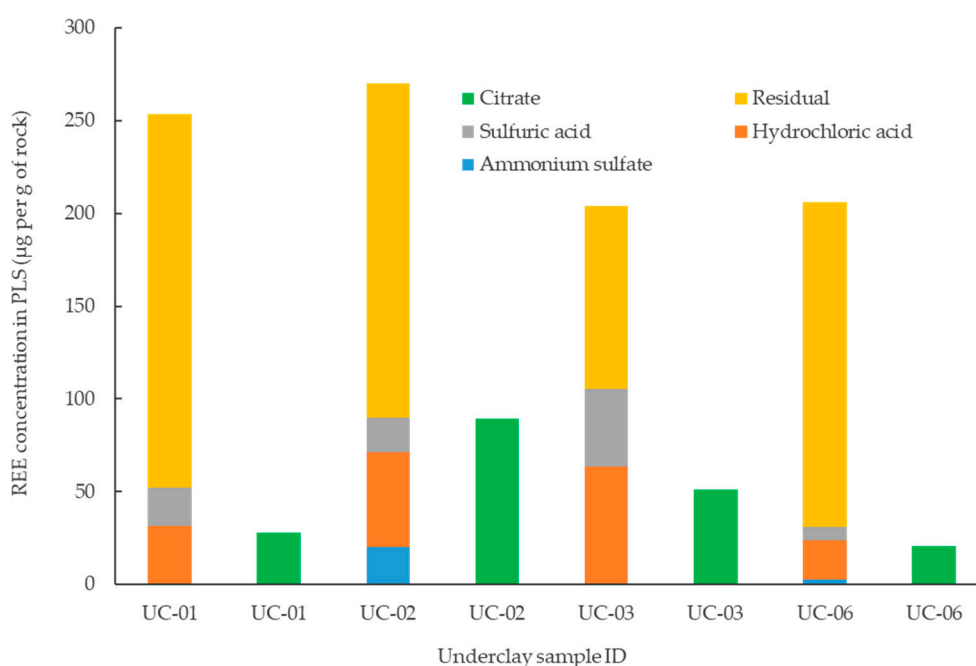


Figure 3. Concentration of REE in PLS after leaching with citrate solution and sequential digestion solutions. Concentrations leached into PLS for each step are denoted by the different bar colors. Citrate recovery values are shown as green bars. Values are reported as concentration of element in leached into PLS per gram of material ($\mu\text{g}/\text{g}$).

The results from the benchtop leaching experiments indicates that the citrate anion solution is more effective at recovering potentially ion exchangeable, or easily liberated REE that is present in the clay-rich sample. Additional REE, excess of ion adsorbed, is likely leached via chelation or complexation of the element from the clay or other mineral surface and solubilized into the leachate, presumably as an REE-citrate complex. In samples with less than < 1% ion exchangeable REE (e.g., UC-01, 03, and 06), citrate leached 10× more REE from the underclay than ammonium sulfate or NaCl, both of which are used commonly to recover exchangeable ions from soil and rock (Table S6, Supplementary Materials). One plausible explanation for the greater recovery of REE from citrate + sodium chloride treatment

compared to ammonium sulfate is the effect of solution electrolyte concentration on dispersion of clay grains [31,32].

Table 8. Concentration (in $\mu\text{g/L}$) of Al, Si, Fe, Th, and REE in mineral acid and organic acid PLS generated from leaching of Middle Kittanning underclay (sample UC-02). Values are adjusted to mass of material leached.

PLS Composition	Al	Si	Fe	Th	REE
Mineral acids					
$(\text{NH}_4)_2(\text{SO}_4)$	5.0	1320	<DL	0.1	202
HCl	27,610	35,006	56,860	16	508
H_2SO_4	21,696	19,766	39,230	6	184
Σ Mineral acids + $(\text{NH}_4)_2(\text{SO}_4)$	76,907	56,092	57,252	24	894
Organic acids					
Citrate + NaCl (step 1 of 2)	21,230	13,491	3246	7.0	976
NaCl only (step 2 of 2)	1060	bd	843	0.5	44
Σ Citrate + NaCl	24,520	13,491	4099	7.5	1020
Citrate + $(\text{NH}_4)_2(\text{SO}_4)$	22,860	16,740	3380	18	146

Sodium chloride amended citrate may balance surface charge and increase total dissolved solids (TDS) conductivity in the leachate that may enhance colloid and particle dispersion [32]. We hypothesize that an increase in clay particle dispersion would lead to increased solution-clay grain interaction and higher recovery. However, the citrate anion leaches a greater fraction of REE than simply the exchangeable fraction, determined by $(\text{NH}_4)_2\text{SO}_4$. It is plausible that exchangeable RE concentrations in these samples are low and do not exceed more than 10% and that citrate liberates an additional fraction of the RE that is not exchangeable and not liberated by ammonium sulfate. Future work will be aimed at optimizing the solution in order to determine if additional mechanisms are at work where clay grains or RE mineral bearing phases are more susceptible to solubilization in the presence of citrate, compared to mineral acids or inorganic salts such as ammonium sulfate.

The concentration of REE and gangue elements in the different leachates from tests conducted on the Middle Kittanning underclay (UC-02) are shown in Table 8. The highest concentration of REE was released (during leaching using one single solution) by leaching with 0.1 M citrate solution amended with NaCl (solution RS-2). The high concentration of Al, Si, and Fe released from samples UC-01 and 06 during treatment with RS-2 leach solution indicates some dissolution of the mineral phases in these samples, as Si is not typically present as an exchangeable ion. The presence of weakly crystalline, amorphous phases and water-soluble species may also contribute to the higher release of these elements. Whether or not the solution can leach REE from refractory or phosphatic minerals such as monazite was not clear. Notably, the citrate PLS from leaching of UC-02 contained measurable P. Further testing is required to evaluate the leachability of these phases using a citrate or other organic acid-based solution. The recovery results for the different solutions tested indicate that the organic acid solution Na-citrate buffered citric acid (solution RS-2) leaches a greater mass of REE compared to ammonium sulfate (Table 8 and Figure 4), in some cases citrate leaching exceeds leaching with inorganic mineral acids (see Figure 4 and Tables S4 and S5).

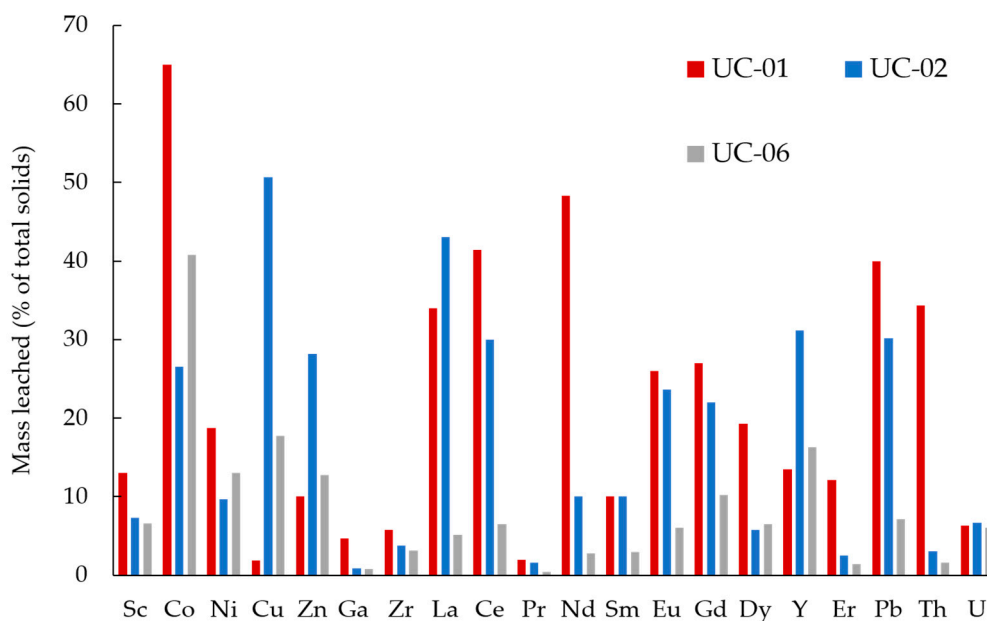


Figure 4. Concentration of REE and other trace metals leached from underclay with 0.1 M citrate + NaCl. Values are reported as the percent of total solids leached from the sample.

Citrate + sodium chloride leaching solution (RS-2) and the other citrate-based solutions tested released a higher concentration of base cations—Al, Si, and Fe—than ammonium sulfate (SEQ-1) but far less than the concentrations of cations released by low-pH inorganic mineral acids (Table 8, Table S3). The ratio of REE to base cations in the leachate accounts for the proportion of REE recovered to the proportion of “contaminants” such as cations Si, Al, and Fe. In recovering 45.9 μg of REE, RS-2, a citrate solution at pH 5, had a REE to base cation ratio of 2.5, compared to a significantly lower value of 0.3–0.2 for the acid and heat-based recovery solutions tested during the sequential extraction. The citrate solution (RS-2) performed best, based on the quantity of REE recovered and the reduction in the concentration of base cations and radioactive Th in the leachate. The citrate + sodium chloride solution, had a significantly higher recovery of REE than $(\text{NH}_4)_2\text{SO}_4$ from all three different underclay materials tested (Table 8, Tables S2 and S3).

The citrate solution leached greater than 30% of the total Ce, La, Nd, Eu, Gd, and Dy from samples 02 and 03. Leaching from UC-06 was significantly less than the other samples, apart from cobalt. For sample UC-02, both Cu, Y, and Pb are abundant in the leachate. Leaching of the radioactive element Th is low in PLS from samples UC-02 and 06, less than 3% of the total Th in the solid. Th leaching from sample UC-01 is nearly 8 \times that from the other samples. The concentration of Th in UC-01 starting solid material was lowest of the samples tested, 14 $\mu\text{g}/\text{g}$, compared to the concentration of Th in UC-02 and 06 which was 22 and 24 $\mu\text{g}/\text{g}$ respectively (see Figure 5 and Table S3). The difference in Th leaching between the samples may be due to the mineral associations of Th in the different clay strata or formations. Notably, there is evidence that Th leaching is minimum, with less than 3% of the total leached from the clay when using citrate for leaching. Reducing Th in leachates, as well as other elements such as U, can help to reduce costs associated with waste disposal and remediation.

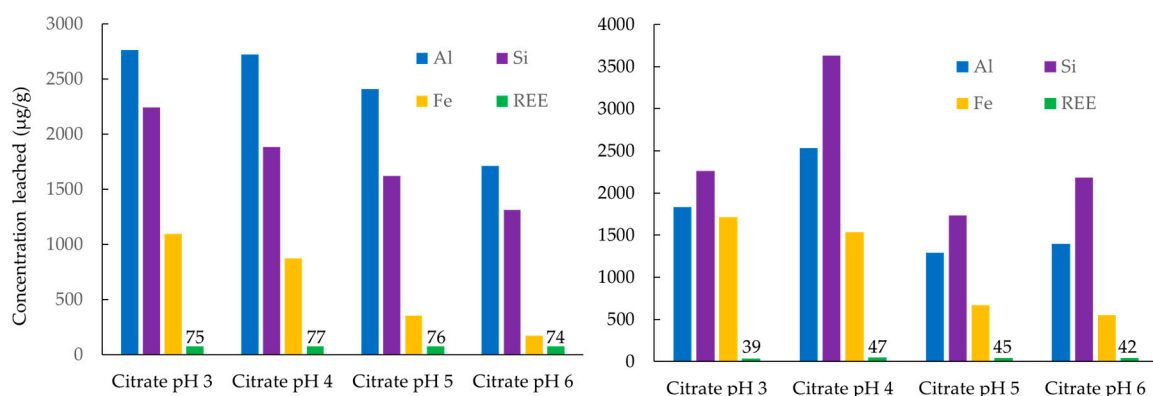


Figure 5. Concentration of Al, Si, Fe, and REE in PLS generated by citrate solution at different pH values for underclay sample UC-02 (left) and UC-03 (right). Values are converted to micrograms of element leached into PLS per gram of underclay ($\mu\text{g/g}$).

We evaluated how the pH of the leaching solution impacts the release of REE and gangue elements from samples UC-02 and UC-03 at a range of pH values from 3 to 6. Figure 5 shows the results from leaching of samples UC-02 and UC-03. For both samples tested, there was no significant change in the concentration of REE leached between pH 3–6. Decrease in the concentration of Al, Si, and Fe in the leachate was observed as pH increased (Figure 5, Table S7). Conversely, calcium in the leachate increased with increasing pH. Sequential acid digestions indicate that a majority of the REE are bound in mineral phases in the residual pool and are not extractable by $(\text{NH}_4)_2\text{SO}_4$, 1 M HCl, or 1.2 M H_2SO_4 . The exceptions are for samples UC-02 and UC-03 which have a greater proportion of REE bound as exchangeable or extractable using hydrochloric and sulfuric acid.

At different pH values, range 3–6, there is a reduction in the concentration of gangue in the leachates (Figure 6). The solution can be pH buffered across a range of pH values from 3–6 which allows for selective leaching of elements from the material. Leaching of non-REE base cations decreases with increasing pH and provides a system to selectively leach REE and minimize leaching of Al, Si, and Fe. Increasing pH should yield greater chelation recovery due to the increase in the number of deprotonated anion sites associated with pKa values for citric acid [12,13]. This is likely due to the monodentate bonding of the REE-citrate complex which is typical of the citrate-metal ion complex [12–14]. This bonding regime is the strongest of the bonds associated with chelation/complexation to carboxylic acid, the functional group on the citrate molecule [14]. There is little change in the concentration of REE in the citrate leachate across pH range 3–6 (see Figure 5, Table S7), which crosses two pKa boundaries for citric acid (e.g., 3.1, 4.7). At pH 4.7, a second carboxylic acid group becomes deprotonated. If this functional group could attract an additional RE ion, there should be a commensurate increase in REE concentration observed between pH 4 and 5 leachates. However, since there is little to no change in REE concentration across the range of pH it is likely the complexation of REE-citrate is more influenced by other factors such as saturation of the clay surface with the solution, dispersion of the clay grains, or amount of carboxylic acid group present (e.g., initial molarity of citrate leaching solution) for chelation and recovery of the metal ions.

The preliminary results from the bench-top experiments indicate that citrate is a chemically effective lixiviant that can be used to generate a PLS from clay-rich sedimentary rock. Presumably, REE and other ionically bound base cations that are present on clay surfaces are solubilized via complexation/chelation with the carboxylic functional group on the citrate anion. Simple chelation/complexation using the citrate anion in solution at pH 5 reduces the potential for dissolution of crystalline mineral phases and concurrent release of elements gangue elements. Such is the case with refractory minerals such as monazite and xenotime that are not only sources of REE but also radioactive elements Th and U. The process presented here is not aimed at leaching of crystalline bound, phosphatic REE. Rather, REE is sorbed to the surface of mineral grains that can be recovered with basic hydrometallurgical leaching.

The citrate PLS generated in the experiments contains a relatively low concentration of gangue elements because of the limited mineral dissolution. The overall economics of the process cannot be assessed at this stage of the research or at the scale of this work. However, future experiments and analysis will be aimed at evaluating the economics of the process including subsequent steps to purify REE from the PLS. Currently there are few processes that have been developed at a higher Technology Readiness Level (TRL) on the extraction and recovery of REE from secondary products and wastes.

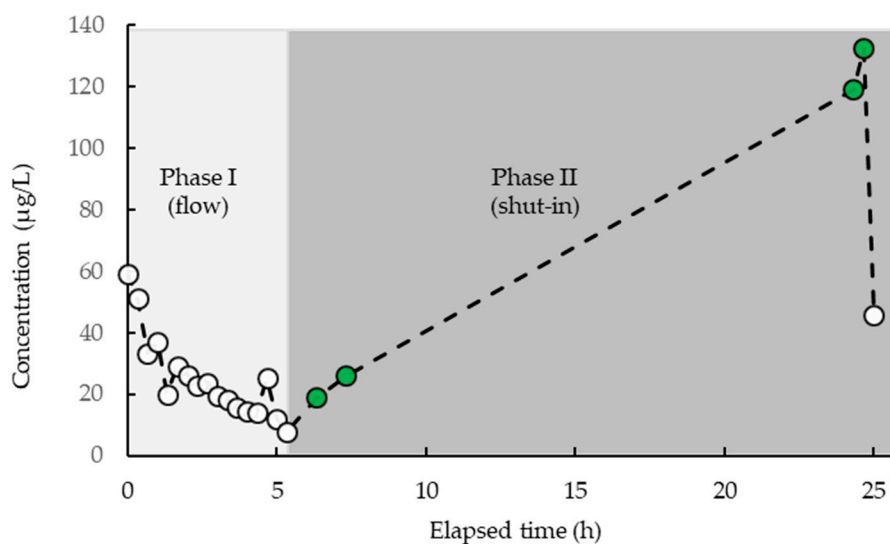


Figure 6. REE concentration (in $\mu\text{g/L}$) in effluent PLS collected during flow-through leaching of Middle Kittanning underclay (UC-02) powder. Black dots denote sampling points taken during continuous flow. Green dots indicate samples taken after various shut-in times.

3.4. Leaching of REE from Powdered Underclay Using Core Flow-Through

An additional set of leaching tests were conducted on the remaining unreacted powders from the benchtop test tube leaching tests. Flow-through leaching reactors (See Supplementary Materials) packed with rock powder were flooded and subjected to pressurized flow at ~ 1600 – 1800 psi to compensate for low porosity and correspondingly low permeability of clay. The highest concentration of REE in effluent leachates occurred during the initial 20–40 min of fluid flow through the powder. Powder reactor runs exhibited lower concentrations of REE released to the fluid and relative to amount of material in reaction vessel. Shut-in periods up to 5 days in some cases recovered equal amounts as continuous flow for 7 h (based on cumulative concentrations). The results indicate that shut-in time may be necessary to fully saturate the material for increased fluid interaction with the surfaces of the clay grains. Peak REE concentrations were also noted to occur within the first 20–40 min of fluid flow, denoted as phase I in Figure 6. Though absolute concentrations increased with increasing fluid shut-in times, the peak REE concentrations were consistently noted to occur within 20–40 min of initializing fluid flow (Figure 6).

Increased recoveries of the REE in the effluent solutions of the underclay powders were evident after increased shut-in times. Peak concentrations increased from the initial start of fluid flow to the samples flowed at 24 h (after ~ 17 -h shut-in period) to the samples flowed at 5 days. An example of the effect shut-in time has on the liberation of REE into solution is shown in Figures 6 and 7.

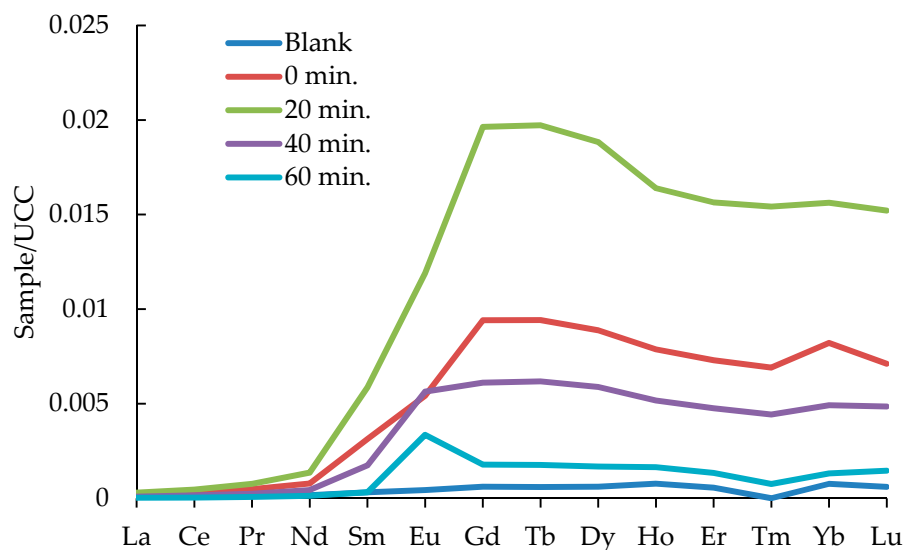


Figure 7. Concentration of REE, normalized to upper continental crust values, in flow-through PLS analyzed at 0, 20, 40, and 60 min.

The highest concentrations of REE were observed in effluents after a 5-day shut-in period. In Figure 6, the initial opening of the reactor, after 5 days, occurs at 0 min. Subsequent measurements were taken at 20, 40, and 60 min after flow was established. The highest concentration of REE in the leachate occurred at 20 min after reestablishing flow (Figure 7). Additionally, the pregnant leach solutions exhibit middle—to heavy—REE enrichments.

Results from these initial flow-through experiments highlight the considerations and parameters that need to be optimized to maximize the extraction of REE from underclay feedstocks using an organic lixiviant such as a sodium citrate solution. The flow-through experiments demonstrate that the initial 20–40 min of flow is the most critical for recovering the highest concentrations of the REE. Additional flow beyond that initial 20–40 min recovers significantly lower concentrations of the REE and may not be economical. The relatively quick release of REE in the first 20–40 min of fluid flow is consistent with our hypotheses that the sodium citrate solution targets the sorbed/colloidal components of the underclays. Increased shut-in times of the fluid with the underclay sample at pressure also led to increased concentrations in the PLS. The highest concentrations of REE in PLS produced came after a 5-day shut-in period. Notably, after these extended shut-in periods, the highest concentrations of the REE were still observed as occurring in the first 20–40 min of fluid flow. We suggest that the mechanism of REE extraction remains the same as in the powder benchtop tests, i.e., desorption from clay surfaces and/or complexation of ions from colloidal phases, but that the additional shut-in time is needed for wetting of micropores and packed grains. These observations are consistent between the powdered samples and the fractured core experiments. However, extraction efficiencies for the flow-through experiment were low, <1% of the total REE content, and likely due to the lower liquid–solid ratio and decreased contact between solution and material due to low transmissivity of the fluid through the material. Increasing the extraction efficiencies for flow-through applications remains an area of active research and further development and testing of a flow-through method that could eventually be employed at the field scale for in situ solution mining is necessary.

3.5. A Method for Recovery of REE from Citrate PLS

In this study a citrate-based al, the subsequent processing, and quantitative recovery of REE from the pregnant leach solution (PLS) is an essential consideration for mining operations and technology economic evaluation of the application. Sorbent capture is a promising technology for the recovery of a high purity REE fraction from PLS, including citrate-based solutions. In conventional mining operations of the REE, the PLS is subjected to a series of purification steps to remove impurities such

as Fe, Al, P, and Th (i.e., gangue elements) before the REE can be recovered [33,34]. While these downstream processes are still an area of active research for the citrate solutions described herein, there are a number of potential pathways that include the use of a novel amine-based sorbent to selectively recover the REE. In order to process the pregnant leachate solution for the recovery of a high purity REE fraction, the leachate is passed over a bed of sorbent material [34]. After leaching, the PLS is passed over a bed of sorbent material [35]. During capture, alkali and alkaline earth elements, as well as the lixiviant, pass through the bed while gangue elements (e.g., Al, Si, Fe, and Th) and REE bind to the bed. Once bound to the sorbent bed, the REE is selectively eluted, away from the gangue elements to produce high purity REE fraction [33,35,36].

In a separate series of laboratory experiments we produced and tested the ability to capture REE from a citrate-based PLS and simultaneously remove gangue elements from the leachate. A citrate PLS—from the leaching of coal prep plant fines with the citrate leaching solution RS-2—was used. The initial, unoptimized sorbent capture test using the citrate PLS showed approximately 60–70% uptake of REE from the feed solution, up through holmium, with a bias toward the light and middle rare earth elements in the unoptimized recovery of bound REE from the sorbent. The overall recovery for the light and middle REE was found to be 80–100% for elements lanthanum to dysprosium, while the recovery ranged from 50–70% for MREE and HREE, with the greatest recovery in this subset occurring with holmium. These results show great promise toward the concentration of REE from a citrate-based PLS generated by leaching of clay-rich geologic material. Future work will be aimed at using the solid sorbent to remove all base metals and other elements from the citrate lixiviant in order to recycle the solution and reuse multiple cycles of leaching. Reuse of the lixiviant during sequential cycles will add cost savings to the process. When coupled with the use of solid polymer sorbents to recover and concentrate REE, citrate leaching may be a promising method for the leaching and concentration of REE from clay-rich coal mine waste rock and coal preparation plant refuse.

4. Conclusions

Underclay associated with coal seams in the Lower Freeport, Middle Kittanning, and Pittsburgh formations contain REE concentrations ranging from 250–353 ppm. Clay minerals such as illite, halloysite, and kaolinite are the predominant clay minerals that make up >55% of the total bulk mineralogy of the rock. The introduction of leaching solutions into underclay rock powder initiates chemical reactions such as ion exchange, hydrolysis, and mineral dissolution that result in the release of ion constituents into the citrate PLS. Bench-top leaching and flow-through experimental results indicate that citrate is a chemically effective molecule for leaching weakly bound REE or other elements of interest from clay-rich sedimentary rock. Rare earths and other metal elements may exist as water soluble, ion exchangeable, or ion/colloidal where the REE is adsorbed to clay or other minerals such as metal oxyhydroxides that are present in the rock. The properties of the citrate molecule provide an added benefit of pH-controlled selectivity against leaching gangue elements from the rock matrix. The process of using organic acid anions for chelation and complexation of target elements is a promising method to leach REE and other critical metals from a variety of different sedimentary lithologies (e.g., underclay, sandstone, and shale) and produced materials such as coal mining waste and coal preparation plant refuse. A chief advantage of the citrate leaching technology is the demonstrated ability to recover REE from feedstocks with minimal release of gangue and radioactive elements, using an environmentally benign and relatively cost-effective leaching solution.

Changes to the physical and/or chemical properties of the clay rock may have both a positive and negative outcome pertaining to the leaching of specific elements from the rock matrix. Bench top powder leach and the flow-through experiments conducted here provide first-order results on the efficacy of organic acid anions for leaching of REE and other elements. Additionally, the results provide observational data on the minimal impact the leaching has on the physical structure of the rock because of the likelihood that there is minimal dissolution of the rock matrix when leaching with citrate at a pH range of 3–6. Continuing work will be aimed toward maximizing the extraction efficiency

of the organic acid-based citrate leaching solution. As described in the methods, a total accounting by mass of the extracted REE from flow-through experiments was not possible but estimates of the extraction efficiency of the system remain low, <1% of the total REE content for the underclay samples. Comparatively, benchtop experiments where powdered underclay samples were reacted with sodium citrate solution at 1% and 10% solids (e.g., Table S5) demonstrated leaching up to ~30% of the total REE. Future work using flow-through experiments will explore parameters such as increasing the leach solution ratio of fluids reacting with the underclay samples, the concentration of the sodium citrate solution, and sampling schemes such as a step-wise shut-in reaction. Information gained from these results and the guided work of future studies will aid in developing a technology economic evaluation of the process to determine costs associated with upscaling this technology for use in larger scale operations.

Supplementary Materials: The following are available online at <http://www.mdpi.com/2075-163X/10/6/577/s1>, Figure S1: Photograph of underclay reaction vessel used in flow-through leaching experiments, Figure S2: Schematic of flow-through apparatus used in powder leaching experiments, Table S1: Concentration of elements in bulk underclay powders used in pH tests, Table S2: Semiquantitative XRD results from random and oriented mounts, Table S3: Results of sequential digest of powdered underclay samples, Table S4: Concentration of trace elements in sequential digest PLS, Table S5: Concentration of elements in PLS from leaching of UC-02 (1 and 10% solids) with 0.1 mol/L citrate and 0.5 mol/L NaCl, Table S6: Concentration of elements ($\mu\text{g/g}$) leached into PLS from underclay samples using citrate solution RS-2, Table S7: Concentration of elements leached from underclay samples UC-02 and UC-03 using citrate solutions buffered to pH 3, 4, 5, and 6, Table S8: Tabulated parameters for particle size distributions of unreacted (initial) underclay samples UC-01, UC-02, UC-03, and UC-06.

Author Contributions: Conceptualization, S.N.M., M.M., and C.V.; methodology, S.N.M.; formal analysis, S.N.M., J.Y. and J.B.; investigation, S.N.M. and J.Y.; resources, J.B., M.M. and C.V.; data curation, S.N.M., and C.V.; writing—original draft preparation, S.N.M., J.Y., J.B., M.M. and C.V.; writing—review and editing, S.N.M., J.Y., J.B., and M.M.; supervision, M.M. and C.V.; project administration, C.V.; funding acquisition, M.M. and C.V. All authors have read and agreed to the published version of the manuscript.

Funding: This work was performed in support of the US Department of Energy's Fossil Energy Crosscutting Technology Research Program. The Research was executed through the NETL Research and Innovation Center's Rare Earth Elements Program. Research performed by Leidos Research Support Team staff was conducted under the RSS contract 89243318CFE000003. **Disclaimer:** This work was funded by the Department of Energy, National Energy Technology Laboratory, an agency of the United States Government, through a support contract with Leidos Research Support Team (LRST). Neither the United States Government nor any agency thereof, nor any of their employees, nor LRST, nor any of their employees, makes any warranty, expressed or implied, or assumes any legal liability or responsibility for the accuracy, completeness, or usefulness of any information, apparatus, product, or process disclosed, or represents that its use would not infringe privately owned rights. Reference herein to any specific commercial product, process, or service by trade name, trademark, manufacturer, or otherwise, does not necessarily constitute or imply its endorsement, recommendation, or favoring by the United States Government or any agency thereof. The views and opinions of authors expressed herein do not necessarily state or reflect those of the United States Government or any agency thereof.

Acknowledgments: We thank Mary Anne Alvin (DOE Rare Earths Technology Manager) and Thomas Tarka (REE FWP Technical Portfolio Lead) for their support. We thank MacMahan Gray (USDOE-NETL) and Brian Kail (LRST) for their time and efforts with sorbent capture tests and analysis, Ward Burgess and Randal Thomas (LRST) for reviewing the manuscript prior to submission.

Conflicts of Interest: The authors declare no conflicts of interest.

References

1. DOE Report. *Report on Rare Earth Elements from Coal and Coal Utilization Byproducts, Report to Congress*; United States Department of Energy: Washington, DC, USA, 2017. Available online: <https://www.energy.gov/sites/prod/files/2018/01/f47/EXEC-2014-000442%20-%20for%20Conrad%20Regis%202.2.17.pdf> (accessed on 29 May 2020).
2. U.S. Geological Survey. *Mineral Commodity Summaries 2020*; U.S. Geological Survey: Reston, VA, USA, 2020; 200p. [CrossRef]
3. Rozelle, P.; Khadikar, A.; Pulati, N.; Soundarrajan, N.; Klima, M.; Mosser, M.; Miller, C.; Pisupati, S. A study on removal of rare earth elements from U.S. coal byproducts by ion exchange. *Metall. Mater. Trans.* **2016**. [CrossRef]

4. Montross, S.N.; Verba, C.A.; Chan, H.L.; Lopano, C. Advanced characterization of rare earth element minerals in coal utilization byproducts using multimodal image analysis. *Int. J. Coal Geol.* **2018**, *195*, 362–372. [CrossRef]
5. Zhang, W.; Yang, X.; Honaker, R.Q. Association characteristic study and preliminary recovery investigation of rare earth elements from fire clay seam coal middlings. *Fuel* **2018**, *215*, 551–560. [CrossRef]
6. Honaker, R.Q.; Zhang, W.; Werner, J. Acid leaching of rare earth elements from coal and coal ash: Implications for using fluidized bed combustion to assist in the recovery of critical materials. *Energy Fuels* **2019**, *33*, 5971–5980. [CrossRef]
7. Appalachian Region Independent Power Producers Association (ARIPPA). 2018 Coal Refuse Whitepaper. Available online: https://arippa.org/wp-content/uploads/2018/12/ARIPPA-Coal-Refuse-Whitepaper-with-Photos-10_05_15.pdf (accessed on 2 April 2019).
8. Lin, R.; Stuckman, M.; Howard, B.; Bank, T.; Roth, E.; Macala, M.; Lopano, C.; Soong, Y.; Granite, E. Application of sequential extraction and hydrothermal treatment for characterization and enrichment of rare earth elements from coal fly ash. *Fuel* **2018**. [CrossRef]
9. Taggart, R.; Hower, J.; Hsu-Kim, H. Effects of roasting additives and leaching parameters on the extraction of rare earth elements from coal fly ash. *Int. J. Coal Geo.* **2018**. [CrossRef]
10. Huang, Q.; Noble, A.; Herbst, J.; Honaker, R. Liberation and release of rare earth minerals from Middle Kittanning, fire clay, and west kentucky No. 13 coal sources. *Powder Technol.* **2018**. [CrossRef]
11. Burckhard, S.R.; Schwab, A.P.; Banks, M.K. The effects of organic acids on the leaching of heavy metals from mine tailings. *J. Hazard. Mater.* **1994**, *41*, 135–145. [CrossRef]
12. Kondoh, A.; Oi, T. Interaction of alkaline earth metal ions with carboxylic acids in aqueous solutions studied by ¹³CNMR spectroscopy. *Z. Für Nat. A* **1998**, *53*, 77–91.
13. Wyrzykowski, D.; Chmurzyński, L. Thermodynamics of citrate complexation with Mn²⁺, Co²⁺, Ni²⁺, and Zn²⁺ ions. *J. Term. Anal. Calorim.* **2010**, *102*, 61–64. [CrossRef]
14. Zabiszak, M.; Nowak, M.; Taras-Goslinksa, K.; Kaczmarek, M.T.; Hnatejko, Z.; Jastrzab, R. Carboxyl groups of citric acid in the process of complex formation with bivalent and trivalent metal ions in biological systems. *J. Inorg. Biochem.* **2018**, *182*, 37–47. [CrossRef] [PubMed]
15. Wang, L.; Lioa, C.; Yang, Y.; Xu, H.; Xiao, Y.; Yan, C. Effects of organic acids on the leaching process of ion-adsorption type rare earth ore. *J. Rare Earths* **2017**, *35*, 1233–1238. [CrossRef]
16. Moldovean, G.A.; Papangelakis, V.G. Recovery of rare earth elements adsorbed on clay minerals: II. Leaching with ammonium sulfate. *Hydrometallurgy* **2013**, *131–132*, 158–166. [CrossRef]
17. Zhi Li, L.; Yang, X. China's rare earth ore deposits and beneficiation techniques ERES2014. In Proceedings of the 1st European Rare Earth Resources Conference, Milos, Greece, 4–7 September 2014; pp. 26–36.
18. Brisson, V.L.; Zhuang, W.; Alvarez, L. Bioleaching of rare earth elements from monazite sand. *Biotechnol. Bioeng.* **2015**, *113*, 339–348. [CrossRef]
19. Shan, X.Q.; Wen, J.J.B. Effect of organic acids on adsorption and desorption of rare earth elements. *Chemosphere* **2002**. [CrossRef]
20. Schumacher, B.; Shines, K.; Burton, J.; Papp, M. *Comparison of Soil Sample Homogenization Techniques*; Lewis Publishers: Chelsea, MI, USA, 1990.
21. Eberl, D.D. *User's Guide to RockJock—A Program for Determining Quantitative Mineralogy from Powder X-ray Diffraction Data, Open-File Report 03-78*; U.S. Geological Survey: Boulder, CO, USA, 2003.
22. Poppe, L.J.; Paskevich, V.F.; Hathaway, J.C.; Blackwood, D.S. *A Laboratory Manual for X-Ray Powder Diffraction, Open-File Report 01-041*; U.S. Geological Survey: Woods Hole, MA, USA, 2010.
23. Sperazza, M.; Moore, J.N.; Hendrix, M.S. High-resolution particle size analysis of naturally occurring very fine-grained sediment through laser diffractometry. *J. Sed. Res.* **2004**. [CrossRef]
24. Peelman, S.; Sun, Z.H.; Siestma, J.; Yang, Y. Leaching of rare earth elements: Past and present. In Proceedings of the 1st European Rare Earth Resources Conference, ERES2014, Milos, Greece, 4–7 September 2014.
25. Bank, T.; Roth, E.; Tinker, P.; Granite, E. *Analysis of Rare Earth Elements in Geologic Samples using Inductively Coupled Plasma Mass Spectrometry*; US DOE Topical Report-DOE/NETL-2016/1794[R]; National Energy Technology Lab. (NETL): Pittsburgh, PA, USA, 2016.
26. Taylor, A.; Blum, J. Relation between soil age and silicate weathering rates determined from chemical evolution of a glacial chronosequence. *Geology* **1995**, *23*, 979–982. [CrossRef]

27. Yang, J.; Montross, S.N.; Britton, J.; Stuckman, M.; Lopano, C.; Verba, C. Microanalytical approaches to characterizing REE Appalachian basin underclays. *Minerals* **2020**, *10*. [[CrossRef](#)]
28. Komnitsas, K.; Modis, K. Geostatistical risk estimation at waste disposal sites in the presence of hot spots. *J. Haz. Mat.* **2009**, *164*, 1185–1190. [[CrossRef](#)]
29. Montross, S.; Verba, C.; Falcon, A.; Poston, J.; McKoy, M. Characterization of rare earth element minerals in coal utilization byproducts and associated clay deposits from Appalachian basin coal resources. In Proceedings of the 34th International Pittsburgh Coal Conference, Pittsburgh, PA, USA, 3–9 September 2019.
30. Hower, J.C.; Groppo, J.G.; Joshi, P.; Dai, S.; Moecher, D.P.; Johnston, M. Location of cerium in coal-combustion fly ashes: Implications for recovery of lanthanides. *Coal Combust. Gasificat. Prod.* **2013**, *5*, 73–78. [[CrossRef](#)]
31. Allen, J.R.L. *Principles of Physical Sedimentology*; Springer: New York, NY, USA, 2012; p. 212.
32. Norrström, A.-C.; Bergstedt, E. The impact of road de-icing salts (NaCl) on colloid dispersion and base cation pools in roadside soils. *Water Air Soil Pollut.* **2001**, *127*, 281–299. [[CrossRef](#)]
33. Gray, M.L.; Kail, B.W.; Wang, Q.; Wilfong, W.C. Stable immobilized amine sorbents for REE and heavy metal recovery from liquid sources. *Environ. Sci. Water Res. Technol.* **2018**. [[CrossRef](#)]
34. Wilfong, C.W.; Kail, B.W.; Wang, Q.; Shi, F.; Shipley, G.; Tarka, T.J.; Gray, M.J. Stable immobilized amine sorbents for heavy metal and REE removal from industrial wastewater. *Environ. Sci. Water Res. Technol.* **2020**, *6*, 1286–1299. [[CrossRef](#)]
35. Wang, Q.; Kail, B.W.; Wilfong, W.C.; Shi, F.; Tarka, T.J.; Gray, M.L. Amine sorbents for selective recovery of heavy rare-earth elements (Dysprosium, Ytterbium) from aqueous solution. *ChemPlusChem* **2020**, *85*, 130–136. [[CrossRef](#)]
36. Wang, Q.; Wilfong, W.C.; Kail, B.W.; Yu, Y.; Gray, M.L. Novel polyethylenimine–acrylamide/SiO₂ hybrid hydrogel sorbent for rare-earth-element recycling from aqueous sources. *ACS Sustain. Chem. Eng.* **2017**, *5*, 10947–10958. [[CrossRef](#)]



© 2020 by the authors. Licensee MDPI, Basel, Switzerland. This article is an open access article distributed under the terms and conditions of the Creative Commons Attribution (CC BY) license (<http://creativecommons.org/licenses/by/4.0/>).